

Dynamic Modeling of Variable Speed Centrifugal Pump Utilizing MATLAB / SIMULINK

Jafar Ghafouri¹, Farid Khayatzadeh H.², Amin Khayatzadeh H.³

¹ Assistant Professor, Mechanical Engineering Faculty, Islamic Azad University, Tabriz Branch, Tabriz, Iran

² M.Sc. Student of Mechatronic Engineering, M.E. Faculty, Islamic Azad University, Tabriz Branch, Tabriz, Iran

³ Lecturer, Mechanical Engineering Faculty, Tabriz University, Tabriz, Iran

(¹gh_jafar@yahoo.com, ²faridkhayatzade@gmail.com, ³khayatzadeh@tabrizu.ac.ir)

Abstract-In this paper a multistage electro pump including a 4 staged stainless steel centrifugal pump, a 4 kW three phase induction motor and two control strategies including constant speed and variable speed methods, is modeled and results are compared with experimental data and Affinity results. The multistage centrifugal pump provides 16 m³/hr flow rate and 58 m_{water} head at BEP (Best Efficiency Point). The model is dynamic and any variation in flow rate results in corresponding variations of electro pump operational parameters. At constant speed mode, the electro pump works at nominal speed immediately after start, regardless to the system characteristics. But, PID speed controller adjusts the rotational speed of the electro pump to the optimized speed regarding to matching the pump working point with the consumption point to save the energy. The model is simulated utilizing MATLAB SIMULINK software with ode45 solver and variable step size.

Keywords- variable frequency drive; frequency control; PID control; BEP; accumulator vessel; multistage centrifugal pump.

I. INTRODUCTION

Regarding to the widespread use of three phase electro pumps in industrial processes under variable loads, there is an obviously important need for a real model of pumping process in order to enhance of efficiency. Many models have been developed by researchers so far. Carsten Skovmose Kallesoe offered the dynamic model of constant speed centrifugal pump in correspondence with "Fault Detection and Isolation in Centrifugal Pumps" in 2005. [1] In this paper both strategies of control including constant speed and PID variable speed have been applied in control sub-model. Pumping system has been set according to fig.1.

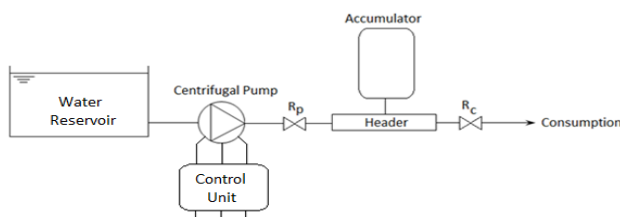


Figure 1. Pumping system set up

Fig.1 shows a centrifugal electro pump, a control unit including speed control strategies, resistances of pump and consumption, a header and an accumulator vessel.

The corresponding modeling diagram in SIMULINK is shown in fig.2. The model includes a three phase voltage source, a controller, a three phase induction motor, a centrifugal pump, a consumption network and sensor sub-models. All parts except sensor and control sub-models are same in both strategies.

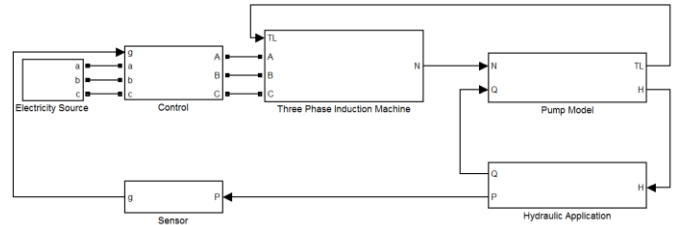


Figure 2. Pumping system modeling in SIMULINK

II. MATHEMATICAL MODELS

A. Three phase voltage source

The three phase voltage source is the provider of AC three phase voltages with constant frequency of ω_e which puts LC filtered three phase voltages on induction motor stator and is modeled using (1) to (3).

$$V_{as} = V_m \cos \omega_e t \quad (1)$$

$$V_{bs} = V_m \cos (\omega_e t + \theta) \quad (2)$$

$$V_{cs} = V_m \cos (\omega_e t - \theta) \quad (3)$$

B. Three phase induction motor

The three phase induction motor works as a converter of electrical energy to mechanical energy that exerts the electromagnetic torque to centrifugal pump. The induction motor is modeled using transformation of fixed abc

coordination to rotating dqo coordination. The equivalent circuit diagram of dqo coordination is shown in Fig.3. The three phase induction motor model maybe formulated as mentioned in (4) to (13). [3]

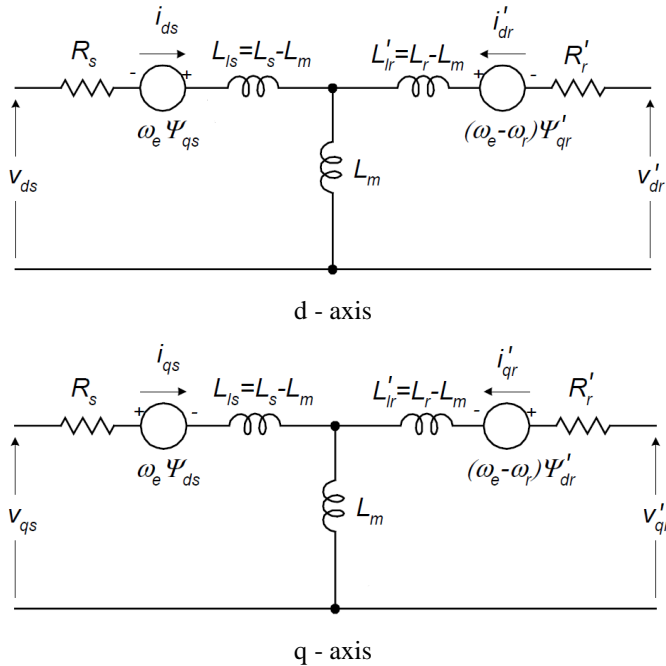


Figure 3. dqo equivalent diagram of induction motor

$$\Psi_{qs} = L_s i_{qs} + L_m i'_{qr} \quad (4)$$

$$\Psi_{ds} = L_s i_{ds} + L_m i'_{dr} \quad (5)$$

$$\Psi'_{qr} = L'_r i'_{qr} + L_m i_{qs} \quad (6)$$

$$\Psi'_{dr} = L'_r i'_{dr} + L_m i_{ds} \quad (7)$$

$$L_s = L_{ls} + L_m \quad (8)$$

$$L'_r = L'_{lr} + L_m \quad (9)$$

$$V_{qs} = R_s i_{qs} + \frac{d}{dt} \Psi_{qs} + \omega_e \Psi_{ds} \quad (10)$$

$$V_{ds} = R_s i_{ds} + \frac{d}{dt} \Psi_{ds} - \omega_e \Psi_{qs} \quad (11)$$

$$V'_{qr} = R'_r i'_{qr} + \frac{d}{dt} \Psi'_{qr} + (\omega_e - \omega_r) \Psi'_{dr} \quad (12)$$

$$V'_{dr} = R'_r i'_{dr} + \frac{d}{dt} \Psi'_{dr} - (\omega_e - \omega_r) \Psi'_{qr} \quad (13)$$

At this investigation, v_{qr} and v_{dr} are set to zero for a squirrel cage induction machine.

$$V_{dr} = 0 \quad (14)$$

$$V_{qr} = 0 \quad (15)$$

The generated electromagnetic torque is modeled as (16).

$$T_e = \frac{3}{2} \left(\frac{P}{2} \right) L_m (i_{dr} i_{qs} - i_{qr} i_{ds}) \quad (16)$$

The rotational speed of rotor is calculated using Newton's second law according to (17).

$$T_e - T_L = J \left(\frac{2}{P} \right) \frac{d\omega_r}{dt} \quad (17)$$

The electric power consumption may be written as (18).

$$P_E = \sqrt{3} \cdot V \cdot I \cdot \cos\phi \quad (18)$$

C. Costant Speed Control Strategy

Constant speed strategy prescribes the pump to run if the pressure drops under the adjusted set point utilizing a pressure switch connected to the header. So, in any pressure drop below the mentioned point, this strategy applies three phase voltages with nominal frequency of ω_e to the induction motor stator, so the electro pump runs at its nominal speed. Hydraulic shock to consumption network and electric shock to electrical network are the important disadvantages of this strategy. The cheaper price at first is the biggest reason for applying this strategy in some pumping systems. Rotational speed in nominal frequency may be obtained from (19).

$$N_s = \frac{120\omega_e}{P} \quad (19)$$

D. Variable Speed Control Strategy

At this strategy, the three phase voltage is applied to induction motor through a three phase VFD (Variable Frequency Drive). The VFD unit changes the AC sinusoidal voltage into DC voltage by passing from a rectifier. After that, the controlled voltage with controlled frequency is applied to IGBT (Insulated Gate Bipolar Transistor) units. The switching frequency and the arrangement are determined by SPWM (Sinusoidal Pulse-Width Modulation). There are several methods for determination of the switching frequency of IGBTs. The frequency control method is based on stability of electromagnetic flux and so, the stability of voltage-frequency ratio may be stated as (20). [8]

$$\frac{V}{f} = 4.44 N \cdot \phi_{max} \quad (20)$$

Fig.4 shows the modeling of variable frequency drive with frequency control in variable speed control strategy.

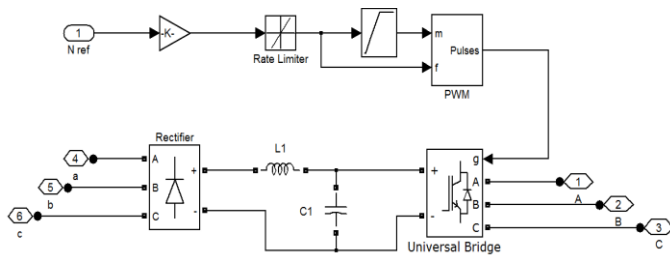


Figure 4. VFD modeling with $V/f = Cte$

The three phase voltage has been made using (20) for the voltage amplitude and PID output speed for the frequency. So, as shown in fig.5, the three phase voltage made with frequency control is compared with a triangular signal. Only, if the voltage amplitude is larger than the triangular signal amplitude, the output signal to the corresponding IGBT is 1. So, the frequency controlled pulses of the IGBTs switching have been made by SPWM. [9]

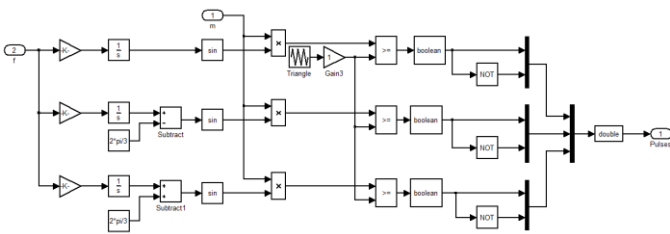


Figure 5. Sinusoidal PWM

Sextuplet switches of IGBTs are controlled by the order of Q_1 to Q_6 to form three phase voltages as shown in figure 6.

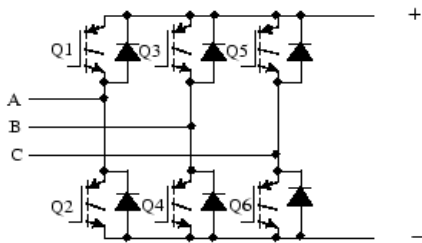


Figure 6. Three phase IGBTs

E. PID controller of rotational speed

The pressure of the header is continuously reported as a feedback of the system and then is converted to the equivalent speed. A PID controller is used to vary the output speed. Output speed of PID controller is the reference speed for VFD.

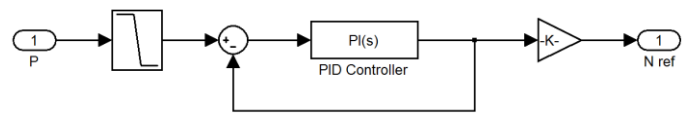


Figure 7. PID controller of speed

F. Centrifugal pump

The centrifugal pump model described by (21), presents a model based on motor dynamics. Effects of pump flow rate and speed are shown in modeling equation. The equation is a form of Riccati equation where a, b and c are determinable constants from pump geometry.

$$H_p = aQ^2 + bQN + cN^2 \quad (21)$$

This equation shows the influence of flow rate and speed on outlet pressure of the centrifugal pump; also it can match with steady - state conditions of pressure versus flow rate curve. The pump torque in a form of similar function of flow rate and speed may be modeled like as (22). [5],[6]

$$T_p = dQ^2 + eQN + fN^2 \quad (22)$$

Frictional torque as a function of friction coefficient and rotational speed may be added to pump torque in order to form the load torque according to (23).

$$T_L = T_p + T_{friction} = T_p + B.N \quad (23)$$

Equations (21) to (23) together form the centrifugal pump model which the flow rate from the consumption network and the rotational speed from the induction motor are its inputs where the head to the consumption network and the load torque to the induction motor are its outputs as seen in fig. 2.

G. Consumption network

As shown in fig.8, the consumption network includes an accumulator vessel, a header and resistances of the pump and consumer which different consumption patterns could be defined for the system using time dependent functions for consumer resistance. The header pressure is measured by a sensor as a criterion and is transmitted to PID controller.

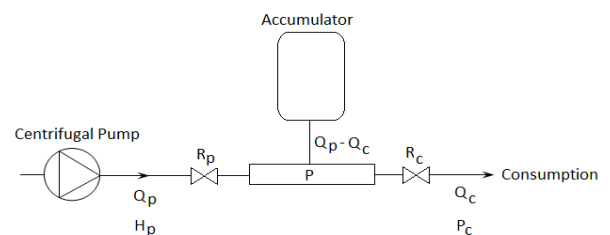


Figure 8. Consumption network

The pump and the consumer resistances may be calculated using (24) and (25).

$$R_p = \frac{\sqrt{H_p - P}}{Q_p} \quad (24)$$

$$R_c = \frac{\sqrt{P - P_c}}{Q_c} \quad (25)$$

An air-water accumulator vessel is made of a metal rigid body and elastic balloon connected to the header for absorbing pressure fluctuations, reducing of hydraulic impacts of the pump start and stop times and finally reducing the pump working time in order to save energy through compensating small pressure drops of the header when it is fully charged. The pressure of the accumulator vessel is calculated using bulk modulus stated in (26) in which the flow rate is the difference of the pump and the consumption flow rates denoted in (27).

$$\dot{P}_{acc} = \frac{\beta}{V_{acc}} (Q_{acc} - \dot{V}_{acc}) \quad (26)$$

$$Q_{acc} = Q_p - Q_c \quad (27)$$

The two main equations used to analyze the gas characteristics are the ideal gas law and the polytropic process equations formulated in (28) , (29).

$$PV = nRT \quad (28)$$

For gas accumulators, an isentropic polytropic process is usually assumed. For an isentropic process n is 1 and for polytropic process n equals with ratio of specific heats. For exact analysis of accumulator vessel, three processes including precharge, charge and discharge processes considered. For gas side of accumulator the polytropic equation may be written as (29).

$$P_g V_g^K = \text{Constant} \quad (29)$$

Differentiating (29) leads to (30).

$$\dot{P}_g V_g^K + KP_g \dot{V}_g V_g^{K-1} = 0 \quad (30)$$

Mass conservation inside accumulator could be written as (31).

$$\dot{P}_{liq} = -\dot{P}_g \quad (31)$$

Substituting of (30) and (31) in (26) results in (32).

$$\dot{P} = \frac{\beta}{V_{liq}} \frac{Q_p - Q_c}{\left[1 + \frac{\beta}{KP} \left(\frac{V_g}{V_{liq}}\right)\right]} \quad (32)$$

Integrating (32) will lead to the header pressure according to (33).

$$P = \int \dot{P} dt \quad (33)$$

H. Pressure sensor

The pressure sensor is only pressure triggered switch adjusted to a desired pressure level at constant speed control strategy where it is an analog pressure transducer which transmits pressure to PID control in variable speed control strategy.

III. RESULTS

The modeled pump is a 4 staged vertical multistage centrifugal pump with 4 kW power, 50 Hz, 380 V AC nominal voltage, 2 poles and 2900 RPM nominal speed squirrel cage three phase induction motor. A 100 liter capacity accumulator vessel connected to pump output and consumption network input assuming that 80% gas and 20% water content at first. Pressure sensor is a 0-10 Bar ranged pressure switch in constant speed control strategy and an analog piezoelectric pressure transmitter with 24 V DC feed voltage and 4-20 mA output current in variable speed control strategy. The applied nominal voltage is 50 Hz, 380 V AC for both strategies. Variable frequency drive is a three phase 4 kW inverter. Fig.9 shows the variations of voltage to nominal voltage ratio versus frequency at frequency control method. At low frequencies, declaration in stator impedance decreases gap flux, so the constant ratio is increased slightly. The head and the torque models constant coefficients have been determined as (34) and (35). Primary conditions and constant parameters have been listed in table. I.

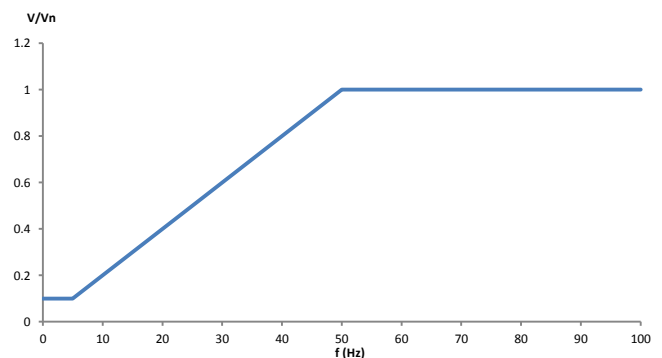


Figure 9. Determining of drive output voltage amplitude in $V/f = C$

Simulation has been done in MATLAB/SIMULINK 7.9.0 (R2009b) software with ode45 solver and variable time step size with discrete simulation type and 1e-6 sampling time.

$$H_p = (-1e - 6)Q^2 + (4.91)Q\omega + (75e - 5)\omega^2 \quad (34)$$

$$T_p = (-500189)Q^2 + (16.90)Q\omega - (1.462e - 5)\omega^2 \quad (35)$$

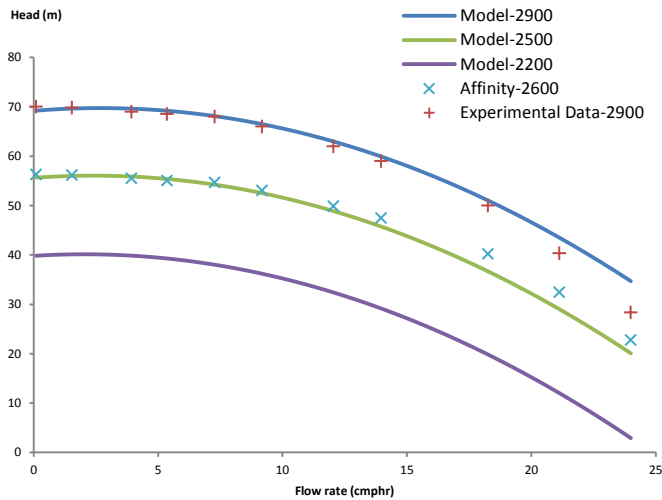


Figure 10. Matching of model results, experimental data and affinity relations

TABLE I. CONSTANT CHARACTERISTICS OF MODELING

Symbol	Description
Head (m)	65 – 32
Flow rate (m ³ /hr)	10 – 24
Number of Stages	4
Nominal Power (kw)	4
Voltage (V)	380
Frequency (Hz)	50
Nominal RPM	2900
Rotor	Squirrel Cage
Number of Poles	2
R _s	1.405
R _r	1.395
L _s (H)	0.005839
L _r (H)	0.005839
L _m (H)	0.1722
J (kg.m ²)	0.093

As shown in fig.10 matching of model results with experimental data and affinity relations implies verifications between model results and steady state conditions in different speeds. [10] Variations of consumption flow rate simulate accumulator vessel charging and then applying of 7 cubic

meters per hour consumption flow rate after fully charging of accumulator vessel.

In fig.11 and fig.12, however the consumption flow rate is at minimum level at first and it takes 25 seconds for charging of the accumulator vessel, for a given consumption flow rate according to the consumption pattern, the constant speed strategy charges and matches with consumption after a hydraulic shock where variable speed strategy matches them without any shock. This is one of the biggest problems of constant speed control strategy and an eye catcher advantage for variable speed control strategy.

Also in fig.13 and fig.14 in which speeds of both strategies have been shown, there is a reduction of speed in variable speed strategy while not any change made in constant speed strategy. The electro pump reached to its nominal speed of 2900 RPM in about 2000 microseconds at constant speed strategy while same electro pump reached to about 2000 RPM in 2.5 seconds at variable speed strategy. Therefore there is an exception for consuming power reduction in variable speed strategy as shown in fig.15 and fig.16.

A PI controller with proportional coefficient of 1 and integral coefficient of 0.9 is applied for PID speed controller at the variable speed control strategy.

With mentioned assumptions and adjustments, there is approximately 5.5 kVA power consumption for constant speed strategy including nominal power and losses where the same electro pump consumes approximately 6 to 7 kVA including nominal power and more losses at variable speed strategy in charging step. After fully charging of accumulator vessel, consumed power drops to 3.5 kVA at constant speed control while it drops to 0.8 kVA at variable speed strategy. After starting and charging of accumulator steps, constant speed strategy power is 4.2 kVA where in same step, variable speed strategy with 62% reduction consumes 1.6 kVA power. This percent could get increased if consumption flow rate decreased to lower level too. So, the variable speed strategy is a better choice for most hydraulic applications from the energy saving view point. High percent's of energy saving rates in variable speed strategy is because of the matching of the consumption and the pump working points. Also, it will be enhanced more if PI coefficients could be adjusted accurately with the system demands. As it could be understood from fig.17 and fig.18, the constant speed strategy generates unnecessary pressure for header about 61 m while at variable speed strategy it is only generated the necessary pressure which is 28 m. Any demand results in corresponding pressure drop, so PID increases drive reference speed carousing corresponding variations in system operational parameters and this demonstrates the dynamicity of modeling. Utilizing this modeling, dynamic, accurate, more controllable and durable with low energy consumption pumping stations could be set up.

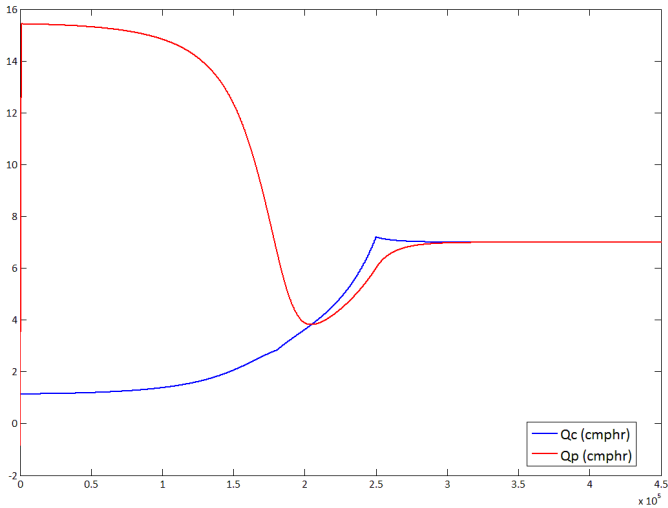


Figure 11. Pump and consumption flow rates in constant speed strategy

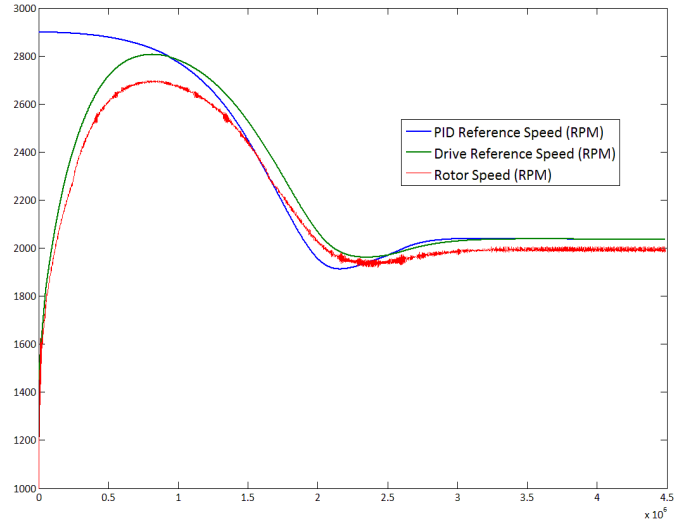


Figure 14. Rotor speed in variable speed strategy

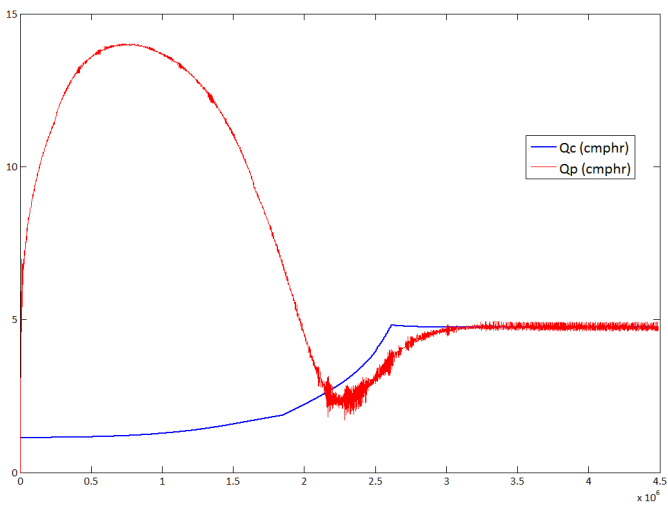


Figure 12. Pump and consumption flow rates in variable speed strategy

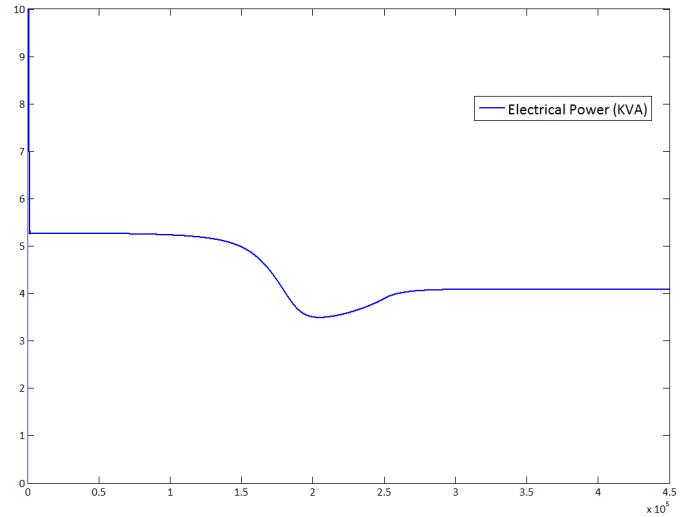


Figure 15. Consumed Electrical Power in constant speed strategy

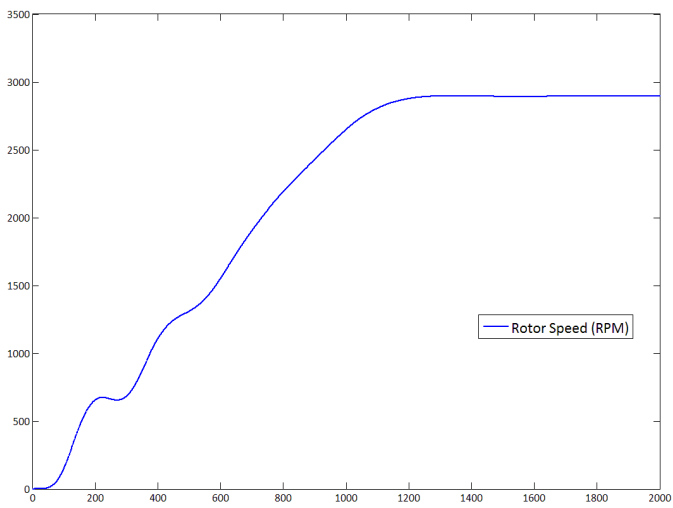


Figure 13. Rotor speed in constant speed strategy

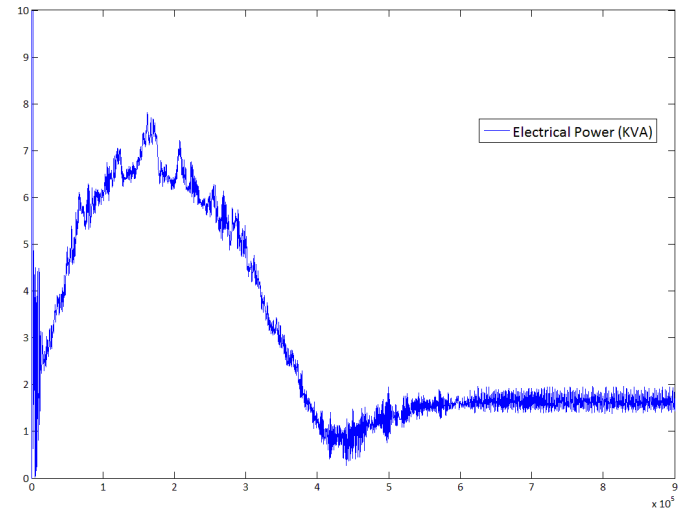


Figure 16. Consumed Electrical Power in variable speed strategy

REFERENCES

- [1] Carsten Skovmose Kallesøe, "Fault Detection and Isolation in Centrifugal Pumps", PhD Thesis, Aalborg University, 2005.
- [2] K.L.Shi, T.F.Chan, Y.K.Wong and S.L.Ho, Modeling and simulation of three phase induction motor using simulink, Department of Electrical Engineering, Hong Kong Polytechnic University, Hong Kong, 1999.
- [3] Krause, P. C., 'Simulation of symmetrical induction machinery', IEEE T rans. Power Apparatus Systems, Vol. PAS-84, No. 11, pp. 1965.
- [4] A. Ansari, D M Deshpande, 'Mathematical Model of Asynchronous Machine' International Journal of Engineering Science and Technology, Vol. 2(5), 2010, 1260-1267.
- [5] Rizwan Uddin, 'Steady state characteristics based model for centrifugal pump transient analysis' Department of Mechanical, Aerospace and Nuclear Engineering, University of Virginia, Charlottesville, USA, 1994.
- [6] Dr.ir. S.A. Miedema, 'Modeling and simulation of the dynamic behavior of a pump/pipeline system' Delft University of Technology, 2010.
- [7] Chee-Mun Ong, "Dynamic simulation of electric machinery using Matlab/Simulink, Prentice Hall, 1998.
- [8] B. Karanay i I, M .F. Rahman and C. Grantham, 'A Complete Dynamic Model for a PWM VSI-fed rotor flux oriented vector controlled Induction Motor Drive using SIMULINK', University of New South Wales, Sydney, NSW 2052, AUSTRALIA, 2009.
- [9] C. Thanga Raj, Member IACSIT, S. P. Srivastava, and Pramod Agarwal, Energy Efficient Control of Three-Phase Induction Motor, International Journal of Computer and Electrical Engineering, Vol. 1, No. 1, April 2009.
- [10] LOWARA PUMPS, SV Series, Vertical Multistage Centrifugal Pumps Catalog, ITT industries.

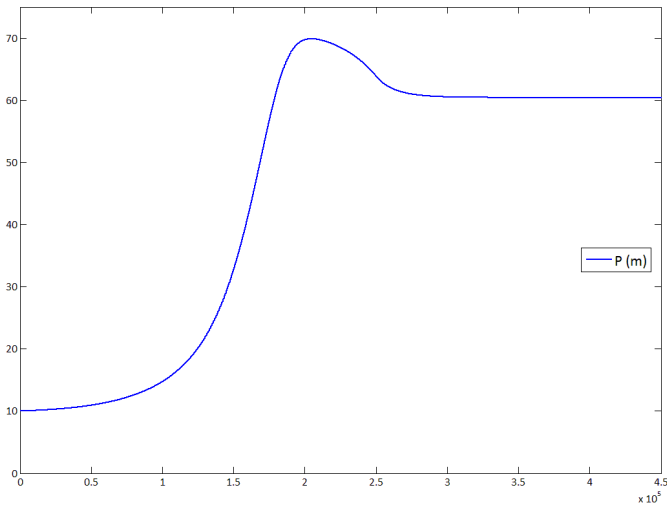


Figure 17. Header pressure in constant speed control strategy

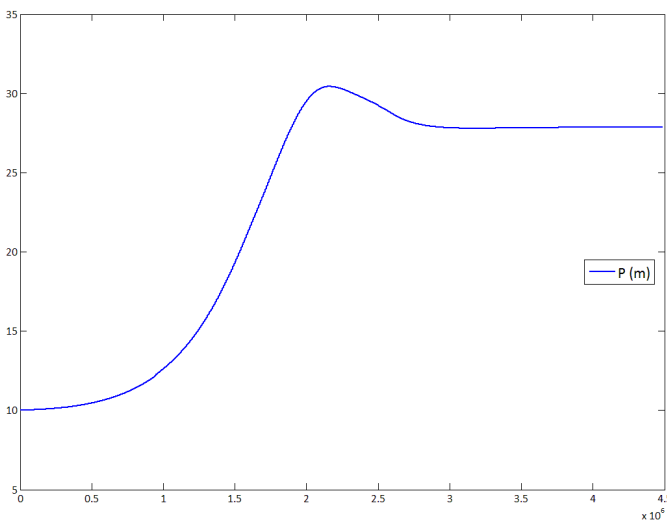


Figure 18. Header pressure in variable speed control strategy

TABLE II. INDUCTION MOTOR SYMBOL DESCRIPTIONS

Symbol	Description
Ψ_{qs}	Stator flux on q-axis
Ψ_{ds}	Stator flux on d-axis
Ψ'_{qr}	Rotor flux on q-axis
Ψ'_{dr}	Rotor flux on d-axis
L_s	Stator inductance
L'_r	Rotor inductance
L_m	Mutal inductance
L_{ls}	Stator leakage inductance
L'_{lr}	Rotor leakage inductance
V_{qs}	Stator voltage on q-axis
V_{ds}	Stator voltage on d-axis
V'_{qr}	Rotor voltage on q-axis
V'_{dr}	Rotor voltage on d-axis